

Detection and control of single proton spins in a thin layer of diamond grown by chemical vapor deposition

Kento Sasaki,¹ Hideyuki Watanabe,² Hitoshi Sumiya,³ Kohei M. Itoh,^{1,4, a)} and Eisuke Abe^{1,5, b)}

¹⁾*School of Fundamental Science and Technology, Keio University, 3-14-1 Hiyoshi, Kohoku-ku, Yokohama 223-8522, Japan*

²⁾*Device Technology Research Institute, National Institute of Advanced Industrial Science and Technology, Tsukuba Central 2, 1-1-1 Umezono, Tsukuba, Ibaraki 305-8568, Japan*

³⁾*Advanced Materials Laboratory, Sumitomo Electric Industries, Ltd., 1-1-1, Koyakita, Itami, Hyogo 664-0016, Japan*

⁴⁾*Center for Spintronics Research Network, Keio University, 3-14-1 Hiyoshi, Kohoku-ku, Yokohama 223-8522, Japan*

⁵⁾*RIKEN Center for Emergent Matter Science, Wako, Saitama 351-0198, Japan*

(Dated: 16 June 2020)

We report detection and coherent control of a single proton nuclear spin using an electronic spin of the nitrogen-vacancy (NV) center in diamond as a quantum sensor. In addition to determining the NV–proton hyperfine parameters by employing multipulse sequences, we polarize and coherently rotate the single proton spin, and detect an induced free precession. Observation of free induction decays is an essential ingredient for high resolution proton nuclear magnetic resonance, and the present work extends it to the atomic scale. We also discuss the origin of the proton as incorporation during chemical vapor deposition growth, which provides an opportunity to use protons in diamond as built-in quantum memories coupled with the NV center.

Hydrogen ^1H atoms are ubiquitous in organic compounds and human body. Proton nuclear magnetic resonance (NMR), including magnetic resonance imaging (MRI), has established itself as an essential tool for molecular structure analysis and clinical diagnosis. Reducing the sample volume down to the atomic scale is tantalizing technological advance that potentially innovates these fields. A leading candidate to achieve this feat, currently under intensive research, is a quantum sensor based on a single nitrogen-vacancy (NV) center in diamond.^{1–6} Indeed, detection of single protons, as well as spectroscopy of single proteins, has been demonstrated using the NV sensor, although the number of reports is still limited.^{7,8} The present work reports detection, as well as coherent control, of elusive single protons via the NV center. We observe free induction decays from a single proton for the first time, bringing the NV-based atomic scale NMR closer to the setting of existing high resolution NMR spectroscopy. Single protons we detect are embedded in a thin layer of diamond grown by microwave plasma assisted chemical vapor deposition (CVD). This has further implications in quantum information processing and materials science; single proton spins in diamond potentially function as quantum memories networking with the NV center qubit,^{9,10} whereas the process of hydrogen incorporation into diamond during the CVD growth is hardly understood.

The diamond sample we examined is a thin layer of diamond CVD-grown on a type-IIa (100) single crystal diamond prepared by the high pressure–high temperature (HPHT) process. The isotopic composition of the substrate is natural abundance ($^{12}\text{C} : ^{13}\text{C} = 98.9\% : 1.1\%$)

with trace amount of nitrogen (< 0.1 ppm).¹¹ Throughout the CVD growth, the microwave power, the chamber pressure, and the substrate temperature were kept at 750 W, 25 Torr, and 800 °C, respectively.¹² The feed gas was a mixture of hydrogen (H_2) and methane (CH_4) with isotopically purified ^{12}C (99.999%).¹³ First, an undoped buffer layer was grown under the condition of $[\text{CH}_4]/[\text{H}_2] = 0.025\%$. The doped layer of a few tens of nanometers was then grown under condition of $[\text{CH}_4]/[\text{H}_2] = 0.5\%$, with the nitrogen-to-carbon ratio of 24%. As a side note, the natural abundance of nitrogen is $^{14}\text{N} : ^{15}\text{N} = 99.63\% : 0.37\%$. We thus can discriminate the NV centers in the CVD layer from those in the substrate unambiguously, by observing an isotope-dependent hyperfine splitting of the $^{15/14}\text{N}$ nuclear spin ($I = \frac{1}{2}$ or 1) intrinsic to the NV center.¹⁴ In reality, we never found ^{14}NV from the present sample.

Our measurement setup is a homebuilt confocal microscope using a 515-nm excitation laser and a single-photon counting module for optically initializing and detecting the electronic spin of the NV center.^{14,15} A copper wire runs across the diamond surface, delivering microwave and radiofrequency (rf) magnetic fields to control the NV electronic spin and the proton nuclear spin, respectively. The $m_S = 0$ and -1 states of the $S = 1$ NV spin were used for quantum sensing, and the microwave frequency was tuned to the corresponding transition. A position-controlled permanent magnet was used to provide a static magnetic field B_0 of 10–40 mT, which was applied parallel to the NV symmetry axis. All the measurements were performed under ambient conditions.

In what follows, we first present a series of data obtained from one particular NV center [labeled as NV1. see the inset of Fig. 1(b) for a fluorescence image], which we will reveal is coupled with a single proton. The data from other NV centers and the discussion on the origin

^{a)}Electronic mail: kitoh@appi.keio.ac.jp

^{b)}Electronic mail: eisuke.abe@riken.jp

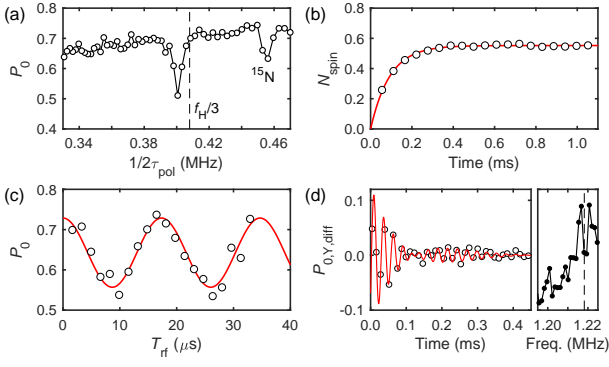


FIG. 2. Control of a single proton nuclear spin. (a) PulsePol spectrum around one-third of the proton Larmor frequency. (b) Transient evolution of polarization transfer. The solid line is an exponential fit. (c) Rabi driving. The solid line is a fit with a sinusoidal function. (d) Free induction decay (left), and its Fourier spectrum (right). The solid line is a fit with a two-component sinusoidal damped oscillation. The dashed line indicates f_p (see the main text for detail).

by the sequence $(\text{PolX})^{20}\text{-L-(PolY)}^{20}\text{-L}_{\text{RO}}$, where the superscript specifies the number of repetitions. The first $(\text{PolX})^{20}$ is to cancel out any nuclear polarization during a preceding run. The NV polarization is recovered by L, and transferred to the nucleus by $(\text{PolY})^{20}$. The decrease in the NV polarization is detected during the second L, which also re-initializes the NV spin for the next run. The spectrum reveals the first dip near $f_H/3 = 0.4080$ MHz (the dashed line) and the second one at 0.4562 MHz. The exact position of the first dip is 0.4006 MHz, which is closer to the one-third of the NMR dip in Fig. 1(a). The second dip has been analyzed as arising from ^{15}N nucleus of the NV center itself, and is not of central interest here.

The degree of polarization transfer can be evaluated quantitatively by the sequence $[(\text{PolX})^{20}\text{-L}]^{20}\text{-}[(\text{PolY})^{20}\text{-L}_{\text{RO}}]^{20}$, where $2\tau_{\text{pol}}$ in PolX/Y is fixed at $2.4960 \mu\text{s} = 3/1.2019 \text{ MHz}$.²⁶ As $(\text{PolY})^{20}\text{-L}_{\text{RO}}$ is repeated, $P_0(n)$, which is P_0 after the n th $(\text{PolY})^{20}$, evolves from $P_0(1) = 0.48$ to the saturation value $P_{0,\text{sat}} = 0.73$, already reached at $n \approx 6$. $P_{0,\text{sat}}$ is primarily determined by the decoherence of the NV spin during the sequence. $P_{0,\text{sat}} - P_0(n)$ quantifies the amount of polarization (in units of \hbar) transferred to the nuclear spin by the n th $(\text{PolY})^{20}$. Therefore, $P_0(n)$ normalized by the integration of $P_{0,\text{sat}} - P_0(n)$ from $n = 1$ to 6 gives the cumulative number of inverted nuclear spins N_{spin} , which is plotted in Fig. 2(b). The solid line is a fit given by an empirical form $N_{\text{spin}} = N_{\text{spin,sat}}(1 - e^{-t/t_c})$, with t the evolution time and t_c the time constant. We find N_{spin} saturate at $N_{\text{spin,sat}} = 0.56$, with $t_c = 93 \mu\text{s}$. While N_{spin} should reach one ideally in the case of a single nuclear spin, the observed $N_{\text{spin}} < 1$ provides a further evidence of the presence of a single proton. A possible reason of N_{spin} not reaching unity is that the polarization rate competes

with the relaxation rate of the nuclear spin.

The polarized nucleus can be driven by an rf pulse. Figure 2(c) demonstrates a nuclear Rabi oscillation recorded by the sequence $[(\text{PolY})^{20}\text{-L}]^{10}\text{-}T_{\text{rf}}\text{-}[(\text{PolY})^{20}\text{-L}_{\text{RO}}]^{10}$, where T_{rf} is the length of an rf pulse with its frequency set at 1.2151 MHz . The $(\text{PolY})^{20}\text{-L}$ block is repeated 20 times during one cycle, so that the nuclear spin is always polarized prior to an rf pulse. In plotting Fig. 2(c), only the first RO data of respective T_{rf} were used (other RO data were to monitor the repolarization process). The sinusoidal fit determines the Rabi frequency to be 57.7 kHz , setting the length of the $\pi/2$ pulse as $T_{\text{rf},\pi/2} = 4.115 \mu\text{s}$. The rf $\pi/2$ pulse induces a free precession of the polarized nuclear spin, which is viewed as a phase-coherent oscillation by the NV center and is measured by the sequence $[(\text{PolY/X})^{20}\text{-L}]^5\text{-}T_{\text{rf},\pi/2}\text{-}[\text{X/2-(XY16-16)-Y/2-L}_{\text{RO}}]^{50}$. The choice of PolY or PolX inverts the sign of the resulting oscillation, as the nuclear spin is polarized to the opposite direction.¹⁵ The detection part after $T_{\text{rf},\pi/2}$ is repeated 50 times in series, with $t_s = N\tau$ in XY16-16 set as $16 \times 411.5 \text{ ns} = 6.584 \mu\text{s}$. X/2 pulses in adjacent blocks are separated by $t_L = 11.840 \mu\text{s}$. In other words, a nuclear spin precession is continuously read out at the “sampling frequency” of $84.46 \text{ kHz} (= 1/t_L)$, undersampled at the 28th order. The readout pulse is Y/2, so that the detection is phase-sensitive: a common feature of high-resolution spectroscopy methods developed recently by several groups.^{27–29} During the continuous readout, the NV spin is either in a superposition of the $m_S = 0$ and -1 states (between X/2 and Y/2, for the duration t_s) or in the $m_S = 0$ state (otherwise, $t_L - t_s$). Therefore, the averaged precession frequency experienced by the NV spin is expected to be $f_p = (f_0 + f_1)/2 \times (t_s/t_L) + f_0 \times (t_L - t_s)/t_L = 1.2182 \text{ MHz}$.^{30,31} Figure 2(d) shows a free induction decay of a single proton nuclear spin thus obtained. The difference between the signals by PolY and PolX are plotted (denoted as $P_{0,Y,\text{diff}}$), and its Fourier spectrum takes into account the undersampling. Remarkably, two peaks appears at $f_a = 1.2173 \text{ MHz}$ and $f_b = 1.2203 \text{ MHz}$, on both sides of f_p (the dashed line). This demonstrates the power of high resolution spectroscopy, which can reveal a fine structure that cannot be done otherwise. The cause of the splitting is discussed below, in conjunction with the origin of the proton.

At this point, we summarize the property of our sample. From fluorescence images of the sample surface [e.g., the inset of Fig. 1(b)], the areal density of the NV centers is estimated to be $3 \times 10^6 \text{ cm}^{-2}$. The fluorescence was obtained only at the surface (far below the depth resolution of our confocal microscope). The most reliable approach to determining the depths of the NV centers in this case is to measure NMR of ensemble protons in an immersion oil.³² In fact, all the measurements, including those for NV1, were performed with an oil immersion objective lens. Out of 25 NV centers measured, 4 showed ensemble proton NMR, 19 no signals, 2 single protons. Typical spectra of the respective cases (labeled as NV2, NV3,

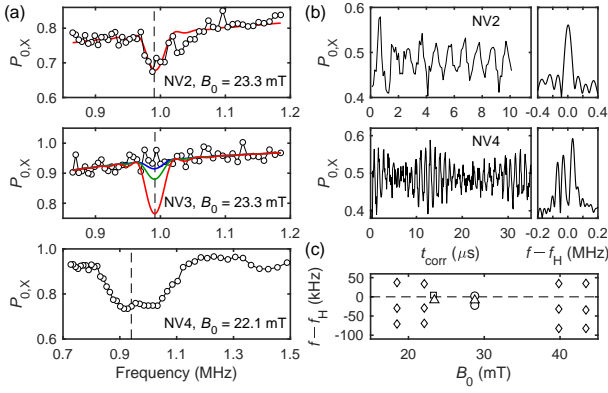


FIG. 3. (a) NMR spectra of NV2 (ensemble, XY16-64), NV3 (no signal, XY16-64), and NV4 (single protons, XY16-16). The dashed lines indicate the proton Larmor frequencies f_H . The solid line in NV2 is a fit with $d_{NV} = 10.3$ nm. The solid lines in NV3 are simulations with $d_{NV} = 10$ (red), 15 (green), and 20 nm (blue). (b) Correlation spectroscopy of NV2 (top panel) and NV4 (bottom panel). Fourier spectra are shown as offsets from the proton Larmor frequencies. (c) The difference between the NMR resonance frequencies and f_H as a function of B_0 . \triangle : NV1, NMR. \circ : NV1, correlation spectroscopy. \square : NV2, correlation spectroscopy. \diamond : NV4, correlation spectroscopy.

and NV4, respectively) are shown in Fig. 3(a). The NMR spectrum of NV2 is fitted by assuming ensemble protons, and the depth of the NV center (d_{NV}) is estimated to be 10.3 nm. See Ref. 32 for detail of the fitting. Correlation spectroscopy confirms a single-component oscillation at the proton Larmor frequency [the top panel of Fig. 3(b)]. NV3 showed no signal. The solid lines are calculated proton ensemble NMR spectra assuming $d_{NV} = 10$, 15 and 20 nm, suggesting that NV3 is located deeper than 20 nm. NV4 exhibited a broad NMR spectrum that is incompatible with proton ensemble. Correlation spectroscopy reveals a multi-component oscillation [the bottom panel of Fig. 3(b)], which arises from couplings to multiple single protons. The large shifts [Fig. 3(d)] suggest a stronger coupling to the NV spin and possibly couplings between protons. A further study on NV4 will be reported elsewhere.³³

As mentioned above, the signal from NV1 is fully explainable from the hyperfine parameters, indicative of deep NV centers. On the other hand, the estimated NV-proton distance ($r = 1.44$ nm) suggests that the observed proton cannot be interpreted as arising from the surface. For instance, the surface of as-grown CVD diamond is terminated by hydrogen. But NMR of the H-terminated surface, if present, would overlap with those of the oil, incompatible with the present observation. We thus conclude that protons were incorporated into diamond during CVD growth. The form of hydrogen within the diamond matrix remains unidentified, but the splitting observed in Fig. 2(d) provides a clue. We speculate it as due to (i) dipolar coupling between ^1H and nearby ^{15}N (I

$= \frac{1}{2}$) or (ii) reconfiguration of ^1H . In the former, if we assume the ^1H - ^{15}N distance to be on the order of the bond length of diamond ($r_d = 0.154$ nm), the coupling strength is roughly estimated as $h\gamma_N\gamma_H\mu_0/4\pi r_d^3 = 3.33$ kHz, close to the observation (γ_N : gyromagnetic ratio of ^{15}N). Complex defects containing both N and H, such as neutral NVH ($S = 0$), may exhibit such a coupling.^{34–36} In the latter, an interstitial ^1H defect could reconfigure its location, temporally changing the distance from the NV sensor. By re-calculating $A_{\parallel,\perp}$ using f_0 deduced from f_a and f_b , and substituting them to the expressions by the dipolar couplings, r is estimated to be 1.57 and 1.41 nm, respectively. This indicates the vibration with the amplitude, again, on the order of the bond length. In this case, the vibration must be slower than the detection sequence, to suppress a motional narrowing effect.

In conclusion, we detected, characterized, and polarized a single proton nuclear spin, and observed its free precession induced by an rf pulse via the NV center. The spatial coordinates r and θ were determined, and the present setup is fully compatible with a protocol to determine the remaining parameter, the azimuthal angle ϕ , as demonstrated by some of the present authors and others recently.^{15,23} Observation of free induction decays is an essential ingredient that makes conventional high resolution proton NMR so powerful. We extend it to the single spin level, and in fact revealed a fine structure in the proton spectrum. The present work thus provides a route toward the atomic scale imaging by employing the state-of-the-art, but rather simple, quantum sensing protocols, which so far have been tested primarily on ^{13}C nuclei in diamond.^{14,15,22–24,30,31,37} The protons we detected and controlled are interpreted to reside in diamond, presumably incorporated during CVD. This points to the possibility to utilize protons in diamond as built-in quantum memories coupled with the NV center. Compared with more common ^{13}C , the higher Larmor frequency of the proton allows for faster operations.

K.S. was supported by the JSPS Grant-in-Aid for Research Fellowship for Young Scientists (DC1), Grant No. JP17J05890. H.W. was supported by the JSPS Grant-in-Aid for Scientific Research (KAKENHI) (B) Grant No. 18H01502. K.M.I. was supported by the JSPS KAKENHI (S) Grant No. 26220602 and (B) Grant No. 19H02547, the JST Development of Systems and Technologies for Advanced Measurement and Analysis (SENTAN), and the Spintronics Research Network of Japan (Spin-RNJ). The data that support the findings of the present work are available from the corresponding author upon reasonable request.

¹H. J. Mamin, M. Kim, M. H. Sherwood, C. T. Rettner, K. Ohno, D. D. Awschalom, and D. Rugar, “Nanoscale Nuclear Magnetic Resonance with a Nitrogen-Vacancy Spin Sensor,” *Science* **339**, 557 (2013).

²T. Staudacher, F. Shi, S. Pezzagna, J. Meijer, J. Du, C. A. Meriles, F. Reinhard, and J. Wrachtrup, “Nuclear Magnetic Resonance Spectroscopy on a (5-Nanometer)³ Sample Volume,” *Science* **339**, 561 (2013).

³C. Müller, X. Kong, J.-M. Cai, K. Melentijević, A. Stacey,

- M. Markham, D. Twitchen, J. Isoya, S. Pezzagna, J. Meijer, J. F. Du, M. B. Plenio, B. Naydenov, L. P. McGuinness, and F. Jelezko, "Nuclear magnetic resonance spectroscopy with single spin sensitivity," *Nat. Commun.* **5**, 4703 (2014).
- ⁴T. Häberle, D. Schmid-Lorch, F. Reinhard, and J. Wrachtrup, "Nanoscale nuclear magnetic imaging with chemical contrast," *Nat. Nanotechnol.* **10**, 125 (2015).
- ⁵S. J. DeVience, L. M. Pham, I. Lovchinsky, A. O. Sushkov, N. Bar-Gill, C. Belthangady, F. Casola, M. Corbett, H. Zhang, M. Lukin, H. Park, A. Yacoby, and R. L. Walsworth, "Nanoscale NMR spectroscopy and imaging of multiple nuclear species," *Nat. Nanotechnol.* **10**, 129 (2015).
- ⁶N. Aslam, M. Pfender, P. Neumann, R. Reuter, A. Zappe, F. F. de Oliveira, A. Denisenko, H. Sumiya, S. Onoda, J. Isoya, and J. Wrachtrup, "Nanoscale nuclear magnetic resonance with chemical resolution," *Science* **357**, 67 (2017).
- ⁷I. Lovchinsky, A. O. Sushkov, E. Urbach, N. P. de Leon, S. Choi, K. De Greve, R. Evans, R. Gertner, E. Bersin, C. Müller, L. McGuinness, F. Jelezko, R. L. Walsworth, H. Park, and M. D. Lukin, "Nuclear magnetic resonance detection and spectroscopy of single proteins using quantum logic," *Science* **351**, 836 (2016).
- ⁸A. O. Sushkov, I. Lovchinsky, N. Chisholm, R. L. Walsworth, H. Park, and M. D. Lukin, "Magnetic Resonance Detection of Individual Proton Spins Using Quantum Reporters," *Phys. Rev. Lett.* **113**, 197601 (2014).
- ⁹P. C. Maurer, G. Kucsko, C. Latta, L. Jiang, N. Y. Yao, S. D. Bennett, F. Pastawski, D. Hunger, N. Chisholm, M. Markham, D. J. Twitchen, J. I. Cirac, and M. D. Lukin, "Maurer room-Temperature Quantum Bit Memory Exceeding One Second," *Science* **336**, 1283 (2012).
- ¹⁰C. E. Bradley, J. Randall, M. H. Abobeih, R. C. Berrevoets, M. J. Degen, M. A. Bakker, M. Markham, D. J. Twitchen, and T. H. Taminiau, *Phys. Rev. X* volume =.
- ¹¹H. Sumiya and S. Satoh, "High-pressure synthesis of high-purity diamond crystal," *Diam. Relat. Mater.* **5**, 1359 (1996).
- ¹²H. Watanabe, D. Takeuchi, S. Yamanaka, H. Okushi, K. Kajimura, and T. Sekiguchi, "Homoepitaxial diamond film with an atomically flat surface over a large area," *Diam. Relat. Mater.* **8**, 1272 (1999).
- ¹³K. M. Itoh and H. Watanabe, "Isotope engineering of silicon and diamond for quantum computing and sensing applications," *MRS Commun.* **4**, 143 (2014).
- ¹⁴E. Abe and K. Sasaki, "Tutorial: Magnetic resonance with nitrogen-vacancy centers in diamond—microwave engineering, materials science, and magnetometry," *J. Appl. Phys.* **123**, 161101 (2018).
- ¹⁵K. Sasaki, K. M. Itoh, and E. Abe, "Determination of the position of a single nuclear spin from free nuclear precessions detected by a solid-state quantum sensor," *Phys. Rev. B* **98**, 121405 (2018).
- ¹⁶T. Gullion, D. B. Baker, and M. S. Conradi, "New, compensated Carr-Purcell sequences," *J. Mag. Res.* **89**, 479 (1990).
- ¹⁷S. Kolkowitz, Q. P. Unterreithmeier, S. D. Bennett, and M. D. Lukin, "Sensing Distant Nuclear Spins with a Single Electron Spin," *Phys. Rev. Lett.* **109**, 137601 (2012).
- ¹⁸T. H. Taminiau, J. J. T. Wagenaar, T. van der Sar, F. Jelezko, V. V. Dobrovitski, and R. Hanson, "Detection and Control of Individual Nuclear Spin Using a Weakly Coupled Electron Spin," *Phys. Rev. Lett.* **109**, 137602 (2012).
- ¹⁹J. M. Boss, K. Chang, J. Armijo, K. Cujia, T. Rosskopf, J. R. Maze, and C. L. Degen, "One- and Two-Dimensional Nuclear Magnetic Resonance Spectroscopy with a Diamond Quantum Sensor," *Phys. Rev. Lett.* **116**, 197601 (2016).
- ²⁰D. Misonou, K. Sasaki, S. Ishizu, Y. Monnai, K. M. Itoh, and E. Abe, "Construction and operation of a tabletop system for nanoscale magnetometry with single nitrogen-vacancy centers in diamond," *AIP Adv.* **10**, 025206 (2020).
- ²¹M. Loretz, J. M. Boss, T. Rosskopf, H. J. Mamin, D. Rugar, and C. L. Degen, "Spurious Harmonic Response of Multipulse Quantum Sensing Sequences," *Phys. Rev. X* **5**, 021009 (2015).
- ²²J. Zopes, K. S. Cujia, K. Sasaki, J. M. Boss, K. M. Itoh, and C. L. Degen, "Three-dimensional localization spectroscopy of individual nuclear spins with sub-Angstrom resolution," *Nat. Commun.* **9**, 4678 (2018).
- ²³J. Zopes, K. Herb, K. S. Cujia, and C. L. Degen, "Three-Dimensional Nuclear Spin Positioning Using Coherent Radio-Frequency Control," *Phys. Rev. Lett.* **121**, 170801 (2018).
- ²⁴M. H. Abobeih, J. Randall, C. E. Bradley, H. P. Bartling, M. A. Bakker, M. J. Degen, M. Markham, D. J. Twitchen, and T. H. Taminiau, "Atomic-scale imaging of a 27-nuclear-spin cluster using a quantum sensor," *Nature* **576**, 411 (2019).
- ²⁵I. Schwartz, J. Scheuer, B. Tratzmiller, S. Müller, Q. Chen, I. Dhand, Z. Wang, C. Müller, B. Naydenov, F. Jelezko, and M. B. Plenio, "Robust optical polarization of nuclear spin baths using hamiltonian engineering of nitrogen-vacancy center quantum dynamics," *Sci. Adv.* **4**, eaat8978 (2018).
- ²⁶J. Scheuer, I. Schwartz, S. Müller, Q. Chen, I. Dhand, M. B. Plenio, B. Naydenov, and F. Jelezko, "Robust techniques for polarization and detection of nuclear spin ensembles," *Phys. Rev. B* **96**, 174436 (2017).
- ²⁷S. Schmitt, T. Gefen, F. M. Stürner, T. Uden, G. Wolff, C. Müller, J. Scheuer, B. Naydenov, M. Markham, S. Pezzagna, J. Meijer, I. Schwarz, M. Plenio, A. Retzker, L. P. McGuinness, and F. Jelezko, "Submillihertz magnetic spectroscopy performed with a nanoscale quantum sensor," *Science* **356**, 832 (2017).
- ²⁸J. M. Boss, K. S. Cujia, J. Zopes, and C. L. Degen, "Quantum sensing with arbitrary frequency resolution," *Science* **356**, 837 (2017).
- ²⁹D. R. Glenn, D. B. Bucher, J. Lee, M. D. Lukin, H. Park, and R. L. Walsworth, "High-resolution magnetic resonance spectroscopy using a solid-state spin sensor," *Nature* **555**, 351 (2018).
- ³⁰M. Pfender, P. Wang, H. Sumiya, S. Onoda, W. Yang, D. B. R. Dasari, P. Neumann, X.-Y. Pan, J. Isoya, R.-B. Liu, and J. Wrachtrup, "High-resolution spectroscopy of single nuclear spins via sequential weak measurements," *Nat. Commun.* **10**, 594 (2019).
- ³¹K. S. Cujia, J. M. Boss, K. Herb, J. Zopes, and C. L. Degen, "Tracking the precession of single nuclear spins by weak measurements," *Nature* **571**, 230 (2019).
- ³²L. M. Pham, S. J. DeVience, F. Casola, I. Lovchinsky, A. O. Sushkov, E. Bersin, J. Lee, E. Urbach, P. Cappellaro, H. Park, A. Yacoby, M. Lukin, and R. L. Walsworth, "NMR technique for determining the depth of shallow nitrogen-vacancy centers in diamond," *Phys. Rev. B* **93**, 045425 (2016).
- ³³K. Sasaki, H. Watanabe, H. Sumiya, K. M. Itoh, and E. Abe, In preparation.
- ³⁴C. Glover, M. E. Newton, P. Martineau, D. J. Twitchen, and J. Baker, "Hydrogen Incorporation in Diamond: The Nitrogen-Vacancy-Hydrogen Complex," *Phys. Rev. Lett.* **90**, 185507 (2003).
- ³⁵J. P. Goss, P. R. Briddon, R. Jones, and S. Sque, "The vacancy–nitrogen–hydrogen complex in diamond: a potential deep centre in chemical vapour deposited material," *J. Phys.: Condens. Matter* **15**, S2903 (2003).
- ³⁶A. M. Edmonds, U. F. S. D'Haenens-Johansson, R. J. Crundace, M. E. Newton, K.-M. C. Fu, C. Santori, R. G. Beausoleil, D. J. Twitchen, and M. L. Markham, "Production of oriented nitrogen-vacancy color centers in synthetic diamond," *Rev. Mod. Phys.* **86**, 035201 (2012).
- ³⁷C. L. Degen, F. Reinhard, and P. Cappellaro, "Quantum sensing," *Rev. Mod. Phys.* **89**, 035002 (2017).